The timescale of adaptation at early and mid-level stages of visual processing

Gaoxing Mei
CAS Key Laboratory of Behavioral Science, Institute of Psychology, Beijing, P.R. China
University of Chinese Academy of Sciences, Beijing, P.R. China
Department of Psychology, Guizhou Normal University, Guiyang, P.R. China

Xue Dong
CAS Key Laboratory of Behavioral Science, Institute of Psychology, Beijing, P.R. China
University of Chinese Academy of Sciences, Beijing, P.R. China

Min Bao
CAS Key Laboratory of Behavioral Science, Institute of Psychology, Beijing, P.R. China

The visual environment changes at multiple timescales. It has been recently demonstrated that visual adaptation is composed of multiple mechanisms operating at differing timescales to accommodate the environmental changes. However, whether multiple adaptation mechanisms correspond to different stages of visual processing remains unclear. To address this issue, in the current study, we compared the timescales of adaptation between the stages of early and mid-level visual processing by tracking the decay of the curvature aftereffect after adaptation to either a compound stimulus or a component stimulus. The results revealed a slower decay for the compound adaptation condition than for the component adaptation condition. Our finding indicates that neural mechanisms for visual adaptation are more sluggish at the mid level than those at the early stage of visual processing.

Introduction

The visual system continuously adapts to the ever-changing visual environment (for reviews, see Kohn, 2007; Webster, 2011, 2015), which is vital for human living (Carbon & Ditye, 2012). For example, adaptation to a shape (e.g., curvature) changes the perception of a subsequent test pattern (Blakemore & Over, 1974; Hancock, & Peirce, 2008; Peirce, 2015).

Recent work has disclosed that multiple mechanisms for visual adaptation operate over differing timescales (Bao & Engel, 2012; Bao, Fast, Mesik, & Engel, 2013; Mei, Dong, Dong, & Bao, 2015; Mesik, Bao, & Engel, 2013; Vul, Krizay, & Macleod, 2008). For example, effects of a longer period of adaptation are rapidly canceled by short exposures to adapters producing the opposite aftereffects (i.e., deadaptation). However, the "spontaneous recovery" of the effects of adaptation is observed when the visual system is again put into the neutral environment. This cannot be accounted for by a single mechanism theory and instead demonstrates the existence of multiple mechanisms for visual adaptation (described in more detail in Bao & Engel, 2012). The findings of multiple adaptation mechanisms support the hypothesis that our visual system may be evolved to accommodate the environment that also changes at multiple timescales. However, the neural substrates underlying the multiple adaptation mechanisms remain largely unknown.

The present study aims to compare the timescales of visual adaptation between the stages of mid-level and early cortical processing by tracking the decay of aftereffects after adaptation to either a curved compound grating pattern or its component gratings. The experimental design is motivated by the previous work about the curved contour adaptation (Hancock, McGovern, & Peirce, 2010; Hancock, & Peirce, 2008; McGovern, Hancock, & Peirce, 2011). To separate the

Citation: Mei, G., Dong, X., & Bao, M. (2017). The timescale of adaptation at early and mid-level stages of visual processing. *Journal of Vision*, *17*(1):1, 1–7, doi:10.1167/17.1.1.

doi: 10.1167/17.1.1 Received July 24, 2016; published January 3, 2017 ISSN 1534-7362

effects of adaptation to local orientations from those to curved contours, Hancock and Peirce (2008) presented two neighboring gratings (compound pattern) in one visual field and alternately presented the component gratings of the compound pattern in another visual field. The effects of adaptation to the compound pattern were found to be greater than those to the component gratings. The authors therefore proposed that the exposure to the compound pattern gave rise to more adaptation in the mid-level visual areas (e.g., V4) than the exposure to the component gratings. Given that multiple timescales of adaptation have been shown to sum linearly (Mesik et al., 2013; Vul et al., 2008), the decay rate of adaptation to the compound pattern should be accordingly influenced by the timescale of the mid-level visual adaptation more than the decay rate of adaptation to the component gratings. Therefore, a slower (or faster) decay rate in the compound adaptation condition than in the component adaptation condition would suggest slower (or faster) timescale of adaptation in the mid-level visual areas than in the early visual areas.

The current results showed that the aftereffects decayed more slowly in the compound condition than in the component condition, suggesting slower adaptation mechanisms for the mid-level than for the early stage of visual processing.

Methods

Participants

Fifteen naïve students (seven women, 18–24 years old, mean age 21), with normal or corrected-to-normal vision, participated in the present experiment. All subjects gave their informed consent prior to the participation and were paid after completing the experiment. The experimental procedure was approved by the Institutional Review Board of the Institute of Psychology, Chinese Academy of Sciences, and conformed to the Code of Ethics of the World Medical Association.

Apparatus

Stimuli were presented on a gamma-corrected CRT monitor, with a resolution of 1,024 × 768 pixels, a refresh rate of 85 Hz, and a mean luminance of approximately 40 cd/m^2. The monitor was driven by a Bits# video card (Cambridge Research Systems, Rochester, UK) and calibrated using a Photo Research PR-655 spectrophotometer. To calibrate the display, gamma curves were measured and inverted with a look-up table. Subjects' heads were steadied in a chin rest. They observed the screen at the distance of 57 cm in a dark room. The experiment was coded using the Psychophysics Toolbox for MATLAB (Brainard, 1997; Pelli, 1997).

Stimuli

All stimuli were generated in the similar manner as in Hancock et al. (2010) and McGovern et al. (2011). In the compound condition, the contour stimuli were composed of two luminance modulated sinusoidal gratings oriented ±70°. These two rectangular patches (Gabor A: 70° and Gabor B: −70°) subtended 10° × 5°, with each patch presented in a Gaussian envelope whose standard deviation was 0.83° and 1.66° in the vertical and horizontal direction, respectively. The adapters with a V-shape contour were created by combining the right half of Gabor A and the left half of Gabor B. This formed an ellipse (10° × 5° visual angle; see Figure 1A). The reference stimuli were the same size as the adapters but made of two horizontal Gabor patches. All stimuli were centered at 6.5° to the left or right of the central fixation on the horizontal meridian. In the component condition, the component Gabors (right half of Gabor A or left half of Gabor B) and their corresponding half of reference stimuli were presented at the same location as in the compound patch condition (see Figure 1B). The spatial frequency of gratings was 1.1 cycles per degree. To obtain the continuous contour, the spatial phase of the stimuli was aligned (e.g., 1/3 π for Gabor A, 5/3 π for Gabor B) and was randomly sampled from 20 phases every 100 ms. All stimuli were presented with 98% contrast.

Procedure

Each session included three stages: a 90-s "baseline" period without adapters (1.5 s for each trial), a 208-s "adaptation" period (2.6 s for each trial), and a 270-s "posttest" period without adapters (1.5 s for each trial).

There were two adapter configurations (see Figure 1). In each trial, the adapter presentation lasted for 2 s. In the component condition, the right half of Gabor A was alternated with the left half of Gabor B every second, which temporally formed a V-shape pattern. The order for presenting the two components was randomized across trials. In the compound condition, the right half of Gabor A and the left half of Gabor B were simultaneously presented for 1 s to form the spatial V-shape pattern, which was alternated with a blank field every second. The order for presenting the adapter and the blank field was also randomized across trials.

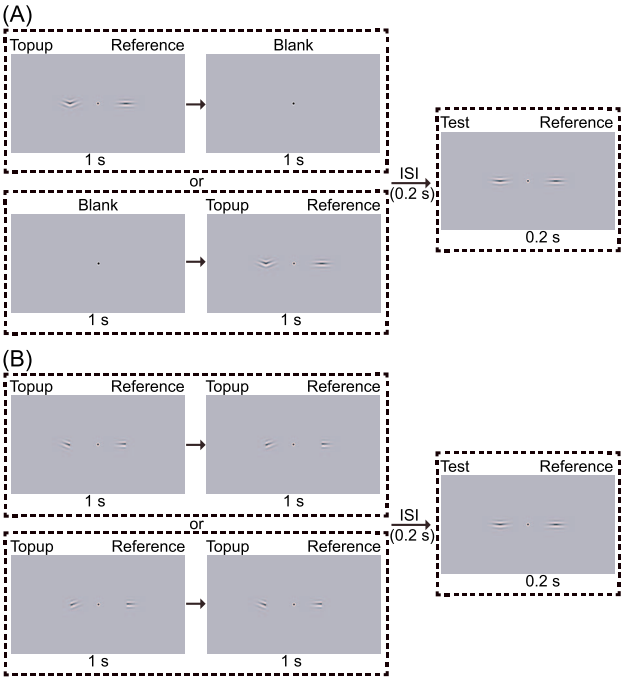

Figure 1. Procedures of (A) the compound condition and (B) the component condition. (A) The top-up compound stimulus lasting for 1 s alternated with a 1-s blank field, followed by a 0.2-s blank interstimulus interval, and then the test stimulus was presented for 0.2 s. The angle of the test stimulus was varied according to a one-down, one-up staircase procedure, and the reference stimulus was kept horizontal. (B) Two component Gabors, which formed the V-shape contour, were presented alternately for 1 s, followed by a 0.2-s blank field interstimulus interval. Subjects reported the orientations of the curvature for the test stimuli (upward or downward) by pressing one of the two buttons (two-alternative forced choice).

In each trial of the adaptation period, after 2 s of adapter presentation and a 200-ms blank interstimulus-interval, the test stimuli were presented for 200 ms. The next trial started after another 200-ms blank field. During the baseline and posttest periods, only the test stimuli were presented for 200 ms, and the blank interval between every two trials was 1300 ms.

The contour angle of the testing stimulus for each trial was varied in a one-down, one-up staircase procedure. Subjects had to judge whether the orientations of curvature for the test stimuli were upward or downward relative to the reference stimuli by pressing one of the two buttons (two-alternative forced choice). They were instructed to keep the central fixation throughout the session. The initial step size of each staircase was 1.5°. It decreased to 1° after three reversals and 0.5° after another three reversals. The adapters were presented to the right hemifield for six sessions and to the left hemifield for an additional six sessions in each condition. At the beginning of each session, subjects were cued on which hemifield test stimuli would be presented. A 1-hr break was required between two successive sessions.

Analysis

Tilt aftereffect (TAE) was defined as the amount of physical tilt required to make the test stimuli perceptually equate to the reference stimuli (point of subjective equality). The baseline of each session was calculated by averaging the last 10 reversals in the baseline period. To normalize the data, this baseline was subtracted from the whole time series. The time series were then interpolated at a 1.5-s sample interval for the baseline and posttest periods and at a 2.6-s sample interval for the adaptation period. Average time courses of TAE for each condition of each subject were obtained by averaging the interpolated time series across sessions. To inspect the time courses of the posttest period for the two conditions, the normalized average time courses were calculated by dividing the TAE at each time point by the maximum adaptation effects, which were defined as the average TAE within the last 40 s of the adaptation period. For each subject, the average time courses of TAE were fitted with a single exponential model as follows (Ho & Berkley, 1988; McLean & Palmer, 1996):

For the adaptation period:

$$y = y_0 \cdot (1 - e^{-t/\tau_1})$$

For the posttest period:

$$y = y_0 \cdot e^{-t/\tau_2}$$

where y_0 is the amplitude of the function and τ_1 and τ_2 are the time constants in the adaptation period and the posttest period, respectively. The fitting was performed using the MATLAB fminsearch function and the least-squares method. A paired t test was performed to compare the time constants for the compound and component conditions. The effect size (Cohen's d) for each comparison was also computed (Cohen, 1992).

Results

The baselines were not significantly different between the two adaptation conditions, $t(14) = -1.12$, $p > 0.25$, compound: 0.25°, component: 0.29° (see Supplementary Table S1 for the individual data in the Supplementary Materials). Therefore, to inspect the adaptation effects more directly, the baselines were subtracted in the following analysis.

Significant adaptation effects were observed for both conditions: compound, $t(14) = 11.88$, $p < 0.001$, $d = 3.07$; component, $t(14) = 12.94$, $p < 0.001$, $d = 3.34$.

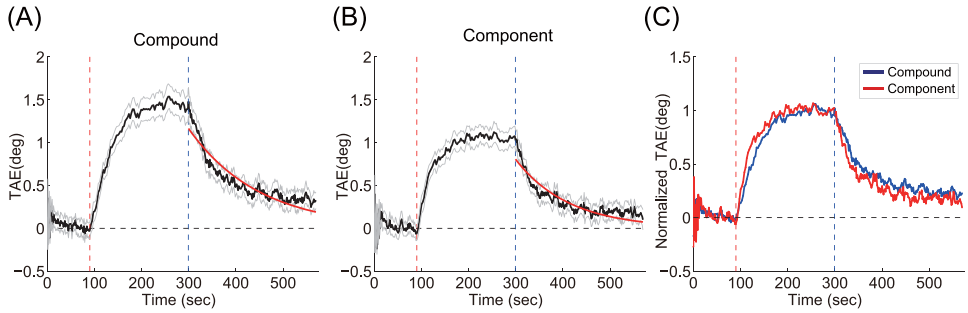

Figure 2. (A, B) Grand average time courses for the compound and component conditions. To evaluate the adaptation effect, the average tilt of the last 10 reversals in the baseline period was subtracted from the whole time series in each session. The black curves indicate the grand average time courses for the tilt aftereffect (TAE), and the gray curves correspond to ±1 standard error of the grand mean. The two vertical dashed lines denote the starting times of the adaptation and posttest stages, respectively. The red curves represent the fitting curves in the posttest stage. (C) Grand average time courses were replotted with the normalized time courses of TAE for ease of visually comparing the two conditions. TAE was normalized by dividing by the maximum adaptation effects, which were defined as the average TAE within the last 40 s of the adaptation period.

Replicating the previous findings (Hancock & Peirce, 2008; McGovern et al., 2011), the adaptation effects in the compound condition were stronger than those in the component condition (see Figure 2A, B): $t(14) = 6.09$, $p < 0.001$, $d = 1.57$; compound, 1.69° ± 0.55°; component, 1.32° ± 0.40°. (See Supplementary Figure S1 in the Supplementary Materials for the grand average time courses without subtracting the baselines.) It is believed that this result reflected that more mid-level visual areas (e.g., V4) encoding the contour information were involved during the compound adaptation relative to the component condition (Hancock & Peirce, 2008; Pasupathy & Connor, 1999).

To examine if there were any residual effects across sessions, we analyzed the changes of the baselines over sessions in a day but failed to observe any significant results: the first two sessions, $t(14) = -0.10$, $p > 0.25$; the first three sessions, $F(2, 42) = 0.33$, $p > 0.25$; the first four sessions, $F(3, 56) = 0.09$, $p > 0.25$. These results indicated that the residual effects observed at the end of each session eventually decayed after a 1-hr break. Therefore, the residual effects from a previous testing can be negligible.

The exponential model fitted the grand average data well, accounting for more than 85% of the total variance of the data (see Supplementary Table S2 in the Supplementary Materials for the quality of fitting on the individual data). The results showed that for both the adaptation and posttest periods, the time constants were larger in the compound condition than in the component condition—adaptation period, $t(14) = 3.59$, $p < 0.01$, $d = 0.93$; τ_1(compound), 45 ± 14 s; τ_1(component), 31 ± 10 s; posttest period: $t(14) = 2.49$, $p < 0.05$, $d = 0.64$; τ_2(compound), 170 ± 94 s; τ_2(component), 128 ± 70 s. (See Supplementary Table S3 for the individual data in the Supplementary Materials.) These results revealed longer-term adaptation mechanisms in the mid-level (e.g., V4) than in the early visual areas.

It should be noted that in the exponential function, y_0 is in theory independent of the time constant parameter τ. However, to ensure the validity of using the exponential fitting, it is important to verify in the data whether the magnitude is indeed independent of the decay rate. Therefore, we performed a correlation analysis in which the half-life—the time required for the adaptation effect to decline to half of its value in the beginning of the posttest—was used to represent the decay rate. The half-life is a relatively fair index to evaluate the decay rate, because it is free of any hypothetical models. For each subject, the average time course of TAE was first smoothed using a method of five-point moving average to reduce the noise. The magnitude of the adaptation effect was defined as the mean value within the last 40 s of the adaptation period on this smoothed time course, whereas the half-life corresponded to the time required for the adaptation effect to reduce to half of the magnitude. However, we found no significant correlations between the magnitude of the adaptation effect and the half-life (compound: $r = 0.07$, $p > 0.25$; component: $r = -0.09$, $p > 0.25$), suggesting that larger adaptation effect did not necessarily lead to slower decay. Accordingly, the results did not support the alternative explanation that the differences in the decay were a consequence of the different magnitudes of adaptation effects.

As shown in Figure 2, the optimal fits of the amplitude appeared to be undershooting the actual initial value in the posttest period, possibly because the initial values (y_0 and τ) were free to vary when fitting the data. One way to avoid this undershoot is to keep the y_0 constant (i.e., use actual initial value). We therefore fitted the data again with such a one-parameter exponential model and then compared it with the two-parameter exponential model by running

an Akaike's information criterion (AIC) test (see Supplementary Figure S2 in the Supplementary Materials for the fitting results and Supplementary Table S4 for the individual data). Usually, the model with the minimum AIC value is deemed to be the preferred model. The AIC testing results showed that the two-parameter exponential model had lower AIC values (compound: AIC = −827.91; component: AIC = −914.29) than the one-parameter exponential model (compound: AIC = −730.69; component: AIC = −828.19), suggesting that the two-parameter exponential model was a better choice to fit our data.

Discussion

Consistent with the previous reports using the compound adaptation paradigm (Hancock & Peirce, 2008; McGovern et al., 2011), the current study showed that the magnitude of the adaptation effect was greater in the compound adaptation condition than in the component adaptation condition. These results provide additional evidence that the curvature detectors in the mid-level visual areas are responsible for the perceptual grouping of edges. More important, we measured and compared the time courses for both the adaptation and decay for the two conditions. This offers an opportunity to explore the timescale of the adaptation in the early and mid-level visual processing areas. Because the time constants of the decay functions were found larger in the compound adaptation condition than in the component adaption condition, we propose that adaptation mechanisms are longer term in the mid-level than in the early visual areas.

To our knowledge, there is no single study systematically comparing the decay of adaptation effects in different visual areas along the visual processing hierarchy. Although the decay functions for adaptation in different brain areas have been previously measured in separate work (Albrecht, Farrar, & Hamilton, 1984; Blakemore & Campbell, 1969; Ho & Berkley, 1988; Manookin & Demb, 2006; McLean & Palmer, 1996; Pavan, Marotti, & Campana, 2012), these studies use different experimental parameters, such as adaptation durations, test durations, spatial frequencies, contrasts, testing methods, and so forth. Thus, based on their findings, it is difficult to compare the time constants of adaptation between different visual processing stages. For the first time, we explored the timescales of adaptation mechanisms between different stages of visual processing on human subjects in a single experiment, making the comparison more accurate and fair.

Hierarchy seems to be a basic organizing principle in the brain. In the spatial and temporal domains, hierarchical features of information processing of the brain have been gradually disclosed (Chaudhuri, Knoblauch, Gariel, Kennedy, & Wang, 2015; Dumoulin & Wandell, 2008; Kiebel, Daunizeau, & Friston, 2008). A particular region of the sensory space in which a stimulus can trigger the firing of a neuron is defined as the receptive field of that neuron (Sherrington, 1906). It is well understood that neurons in higher-level brain areas receive many inputs from lower-level brain areas and that spatial receptive fields of the neurons progressively expand along the visual processing streams (Dumoulin & Wandell, 2008; Hubel & Wiesel, 1962; Wallisch & Movshon, 2008). In the temporal domain, mounting evidence has proved the existence of a hierarchy of a progressively longer temporal receptive window (TRW; Honey et al., 2012)—a neuron's TRW is defined as the length of time within which the processing of present sensory information can be affected by prior information (Hasson, Yang, Vallines, Heeger, & Rubin, 2008). Moreover, higher-order brain regions with longer TRW showed slower dynamics (Honey et al., 2012; Stephens, Honey, & Hasson, 2013). To investigate the neurobiological mechanisms of the hierarchical timescales, Chaudhuri et al. (2015) built a large-scale dynamical model in the macaque neocortex. Propagation of the model's response across brain areas can be observed when simulated stimulus input is imposed to the primary visual cortex, and, in particular, progressively longer decay times of autocorrelation along the cortical hierarchy were found. Considering Chaudhuri et al.'s (2015) and Honey et al.'s (2012) theories, our findings can be explained as follows. Adaptation mechanisms in the mid-level visual areas may give more weights to their past states than those in the early visual areas. This makes the former more sluggish, producing longer-term adaptation effects. Future work may compare the time courses among a range of adaptation effects associated with different processing levels of the visual hierarchy (e.g., between the mid- and high-level visual areas) to extend our current conclusion.

One may notice that the effects of adaptation in our experiment failed to decay to the baselines even by the end of the posttest period. By living in a normal visual environment for sufficiently long (e.g., at least 1 hr of rest in our study), the effects may greatly reduce toward the baselines. To our knowledge, a very similar phenomenon was first reported in Wolfe and O'Connell's (1986) study, in which a residual TAE (~30% of the maximum aftereffect) is present at the end of the posttest (240 s, close to our 270 s) in their two longest adaptation duration conditions (180 s and 240 s, close to our 208 s). Wolfe and O'Connell speculate that this long-term aftereffect might reflect some structural change in regard to synaptic plasticity. Our observed residual effect might have similar causes. However,

more evidence is still needed to ascertain the underlying mechanisms.

Another possible solution for comparing the timescale between the early and mid-level visual areas is to adopt a deadaptation paradigm like our previous work (Bao et al., 2013; Mei et al., 2015). In those two studies, the orientation of the adapter remained constant through different adaptation periods where the adapting contrast varied. The results showed a spontaneous recovery in the posttest after deadaptation, which is used to demonstrate the residual effect from a relatively long-term mechanism that survives the short-term deadaptation. We had attempted to adopt this paradigm in a preliminary experiment of the present study. However, Harris and Calvert (1989) have shown that lowering adapting contrasts does not necessarily weaken the TAEs. This was replicated in our pilot experiment. In this regard, the current study opens an alternative way to investigate the timescale of adaptation mechanisms when the deadaptation approach fails to work.

In conclusion, using a psychophysical method, for the first time we showed that the timescale of adaption mechanisms for the mid-level visual areas were substantially slower than those for the early visual areas.

Keywords: compound adaptation, curvature, visual adaptation, mid-level visual processing

Acknowledgments

We are grateful to the anonymous reviewers for helpful suggestions. This research was supported by the Key Research Program of Chinese Academy of Sciences (KSZD-EW-TZ-003) and the National Natural Science Foundation of China (31371030 and 31571112).

Commercial relationships: none.
Corresponding author: Min Bao.
Email: baom@psych.ac.cn.
Address: CAS Key Laboratory of Behavioral Science, Institute of Psychology, Beijing, P.R. China.

References

Albrecht, D. G., Farrar, S. B., & Hamilton, D. B. (1984). Spatial contrast adaptation characteristics of neurones recorded in the cat's visual cortex. *Journal of Physiology*, *347*, 713–739.

Bao, M., & Engel, S. A. (2012). Distinct mechanism for long-term contrast adaptation. *Proceedings of the National Academy of Sciences, USA*, *109*, 5898–5903.

Bao, M., Fast, E., Mesik, J., & Engel, S. (2013). Distinct mechanisms control contrast adaptation over different timescales. *Journal of Vision*, *13*(10): 14, 1–11, doi:10.1167/13.10.14. [PubMed] [Article]

Blakemore, C., & Campbell, F. W. (1969). On the existence of neurones in the human visual system selectively sensitive to the orientation and size of retinal images. *Journal of Physiology*, *203*, 237–260.

Blakemore, C., & Over, R. (1974). Curvature detectors in human vision? *Perception*, *3*, 3–7.

Brainard, D. H. (1997). The psychophysics toolbox. *Spatial Vision*, *10*, 433–436.

Carbon, C. C., & Ditye, T. (2012). Face adaptation effects show strong and long-lasting transfer from lab to more ecological contexts. *Frontiers in Psychology*, *3*(3), 3.

Chaudhuri, R., Knoblauch, K., Gariel, M. A., Kennedy, H., & Wang, X. J. (2015). A large-scale circuit mechanism for hierarchical dynamical processing in the primate cortex. *Neuron*, *88*, 419–431.

Cohen, J. (1992). A power primer. *Psychological Bulletin*, *112*, 155–159.

Dumoulin, S. O., & Wandell, B. A. (2008). Population receptive field estimates in human visual cortex. *Neuroimage*, *39*, 647–660.

Hancock, S., McGovern, D. P., & Peirce, J. W. (2010). Ameliorating the combinatorial explosion with spatial frequency-matched combinations of v1 outputs. *Journal of Vision*, *10*(8):7, 1–14, doi:10.1167/10.8.7. [PubMed] [Article]

Hancock, S., & Peirce, J. W. (2008). Selective mechanisms for simple contours revealed by compound adaptation. *Journal of Vision*, *8*(7):11, 1–10, doi:10.1167/8.7.11. [PubMed] [Article]

Harris, J. P., & Calvert, J. E. (1989). Contrast, spatial frequency and test duration effects on the tilt aftereffect: Implications for underlying mechanisms. *Vision Research*, *29*, 129–135.

Hasson, U., Yang, E., Vallines, I., Heeger, D. J., & Rubin, N. (2008). A hierarchy of temporal receptive windows in human cortex. *Journal of Neuroscience*, *28*, 2539–2550.

Ho, W. A., & Berkley, M. A. (1988). Evoked potential estimates of the time course of adaptation and recovery to counterphase gratings. *Vision Research*, *28*, 1287–1296.

Honey, C., Thesen, T., Donner, T., Silbert, L., Carlson, C., & Devinsky, O., . . . Hasson, U. (2012). Slow cortical dynamics and the accumulation of information over long timescales. *Neuron*, *76*, 423–434.

Hubel, D. H., & Wiesel, T. N. (1962). Receptive fields, binocular interaction and functional architecture in the cat's visual cortex. *Journal of Physiology*, *160*, 106–154.

Kiebel, S. J., Daunizeau, J., & Friston, K. J. (2008). A hierarchy of time-scales and the brain. *Plos Computational Biology*, *4*, 113–123.

Kohn, A. (2007). Visual adaptation: physiology, mechanisms, and functional benefits. *Journal of Neurophysiology*, *97*, 3155–3164.

Manookin, M. B., & Demb, J. B. (2006). Presynaptic mechanism for slow contrast adaptation in mammalian retinal ganglion cells. *Neuron*, *50*, 453–464.

McGovern, D. P., Hancock, S., & Peirce, J. W. (2011). The timing of binding and segregation of two compound aftereffects. *Vision Research*, *51*, 1047–1057.

McLean, J., & Palmer, L. A. (1996). Contrast adaptation and excitatory amino acid receptors in cat striate cortex. *Visual Neuroscience*, *13*, 1069–1087.

Mei, G., Dong, X., Dong, B., & Bao, M. (2015). Spontaneous recovery of effects of contrast adaptation without awareness. *Frontiers in Psychology*, *6*, 1464.

Mesik, J., Bao, M., & Engel, S. A. (2013). Spontaneous recovery of motion and face aftereffects. *Vision Research*, *89*, 72–78.

Pasupathy, A., & Connor, C. E. (1999). Responses to contour features in macaque area v4. *Journal of Neurophysiology*, *82*, 2490–2502.

Pavan, A., Marotti, R. B., & Campana, G. (2012). The temporal course of recovery from brief (sub-second) adaptations to spatial contrast. *Vision Research*, *62*, 116–124.

Pelli, D. G. (1997). The videotoolbox software for visual psychophysics: Transforming numbers into movies. *Spatial Vision*, *10*, 437–442.

Peirce, J. W. (2015). Understanding mid-level representations in visual processing vision. *Journal of Vision*, *15*(7):5, 1–9, doi:10.1167/15.7.5. [PubMed] [Article]

Sherrington, C. S. (1906). Observations on the scratch-reflex in the spinal dog. *Journal of Physiology*, *34*, 1–50.

Stephens, G. J., Honey, C. J., & Hasson, U. (2013). A place for time: The spatiotemporal structure of neural dynamics during natural audition. *Journal of Neurophysiology*, *110*, 2019–2026.

Vul, E., Krizay, E., & Macleod, D. I. (2008). The McCollough effect reflects permanent and transient adaptation in early visual cortex. *Journal of Vision*, *8*(12):4, 1–12, doi:10.1167/8.12.4. [PubMed] [Article]

Wallisch, P., & Movshon, J. A. (2008). Structure and function come unglued in the visual cortex. *Neuron*, *60*, 195–197.

Webster, M. A. (2011). Adaptation and visual coding. *Journal of Vision*, *11*(5):3, 1–23, doi:10.1167/11.5.3. [PubMed] [Article]

Webster, M. A. (2015). Visual adaptation. *Annual Review of Vision Science*, *1*, 547–567.

Wolfe, J. M., & O'Connell, K. M. (1986). Fatigue and structural change: Two consequences of visual pattern adaptation. *Investigative Ophthalmology & Visual Science*, *27*, 538–543. [PubMed] [Article]